

Snowfall in the Alps: Evaluation and projections based on the EURO-CORDEX regional climate models

Prisco Frei¹, Sven Kotlarski^{2,*}, Mark A. Liniger², Christoph Schär¹

¹ Institute for Atmospheric and Climate Sciences, ETH Zurich, 8006, Zurich, Switzerland

² Federal Office of Meteorology and Climatology, MeteoSwiss, 8058 Zurich-Airport, Switzerland

* Corresponding author: sven.kotlarski@meteoswiss.ch

- Supplementary Material -

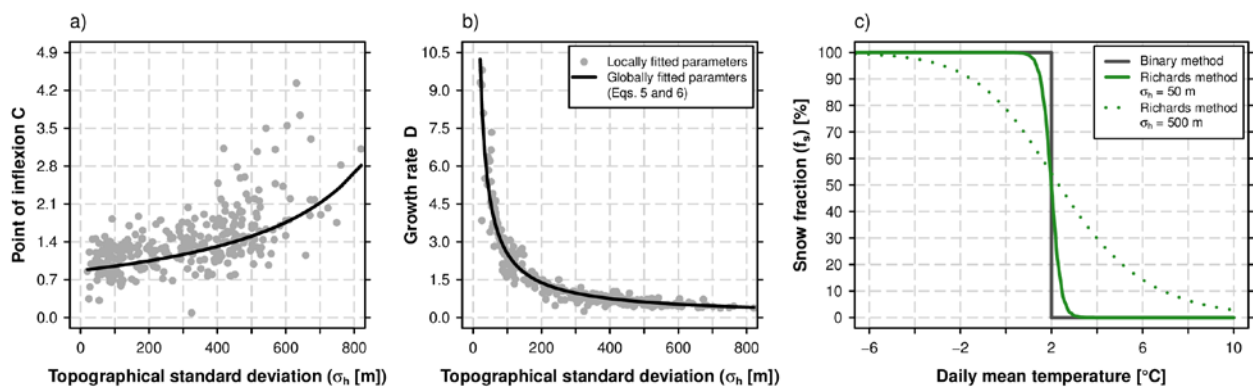


Figure S1 a) and b) Expressing the point of inflexion C and the growth rate D of the Richards equation as a function of the subgrid topographical standard deviation. Grey circles: Fitted parameters for each grid cell in the Swiss domain. Black line: Global fit. c) Example for deriving the daily snow fraction sf based on the binary method with a snow fractionation temperature $T = 2^\circ\text{C}$ (gray line) and based on the Richards method assuming subgrid topographical standard deviations of 50 m (solid green line) and 500 m (dotted green line).

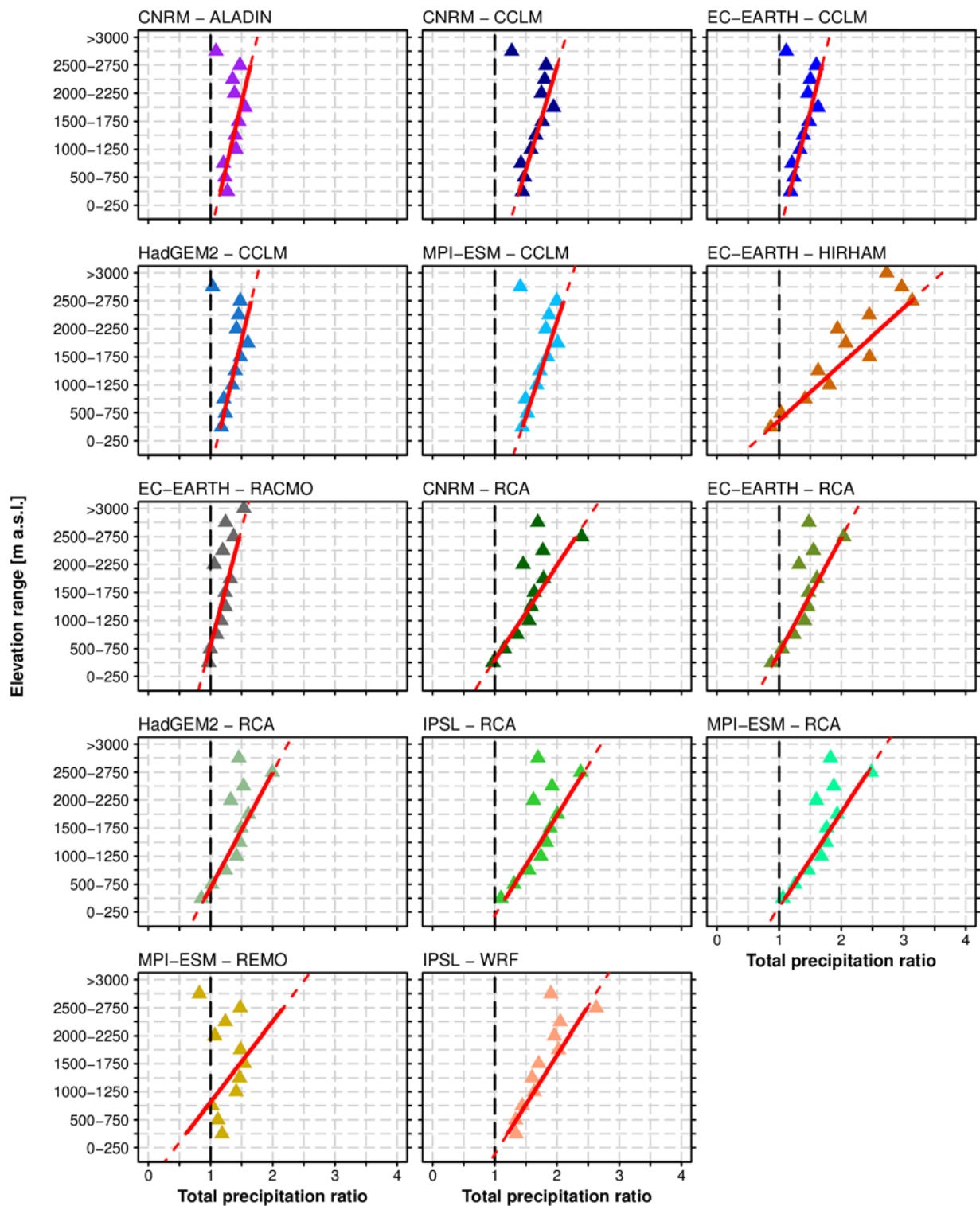


Figure S2: Ratios (RCM simulations divided by observational analysis) of total precipitation sums from September to May in 1971 - 2005 vs. elevation for the Swiss domain. The linear regression line, applied to the ratios for elevations between 250 m a.s.l. and 2750 m a.s.l., is represented by the red line.

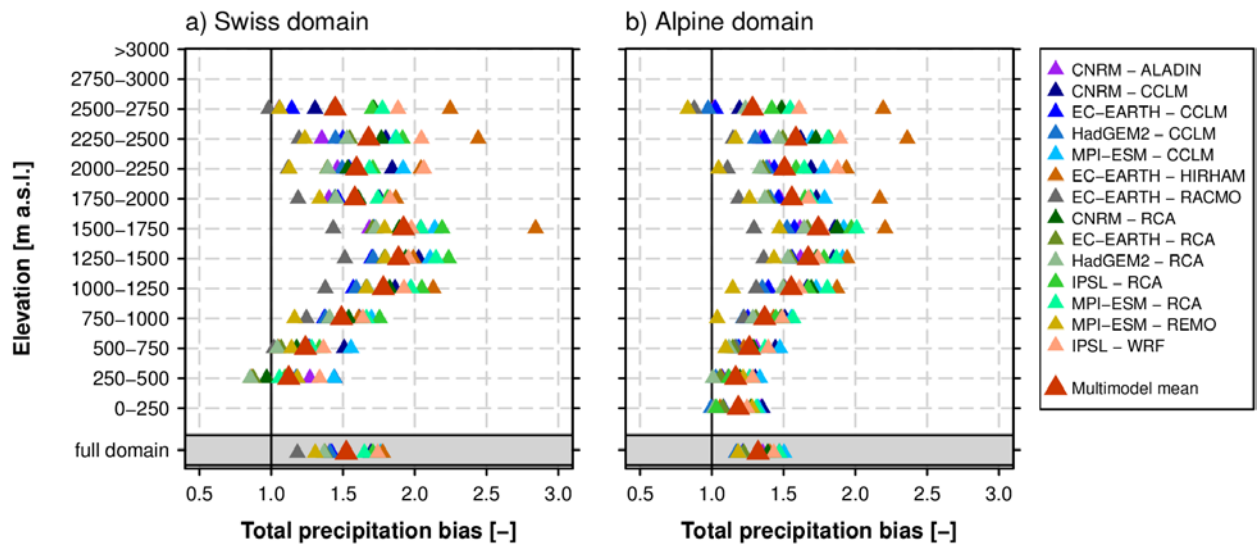


Figure S3: Total winter (SEP-MAY) precipitation bias (expressed as quotient between RCM simulations and observations) in the EVAL period 1971-2005 for individual elevation intervals and for the full domain (lowermost row). Left panel: Swiss domain only. Right panel: Entire Alpine analysis domain (cf. Fig. 1). Observational reference: EOBS version 13.1 (Haylock et al., 2008) on 0.22° interpolated to the 0.11° RCM grid by nearest neighbour interpolation.

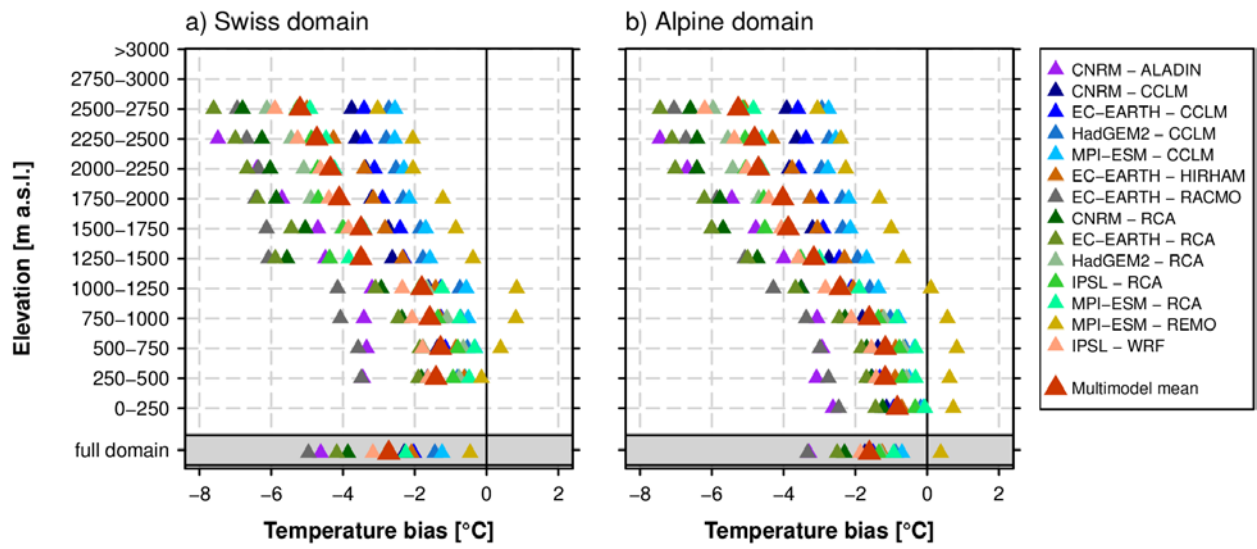


Figure S4: As Figure S3 but for the winter (SEP-MAY) temperature bias.

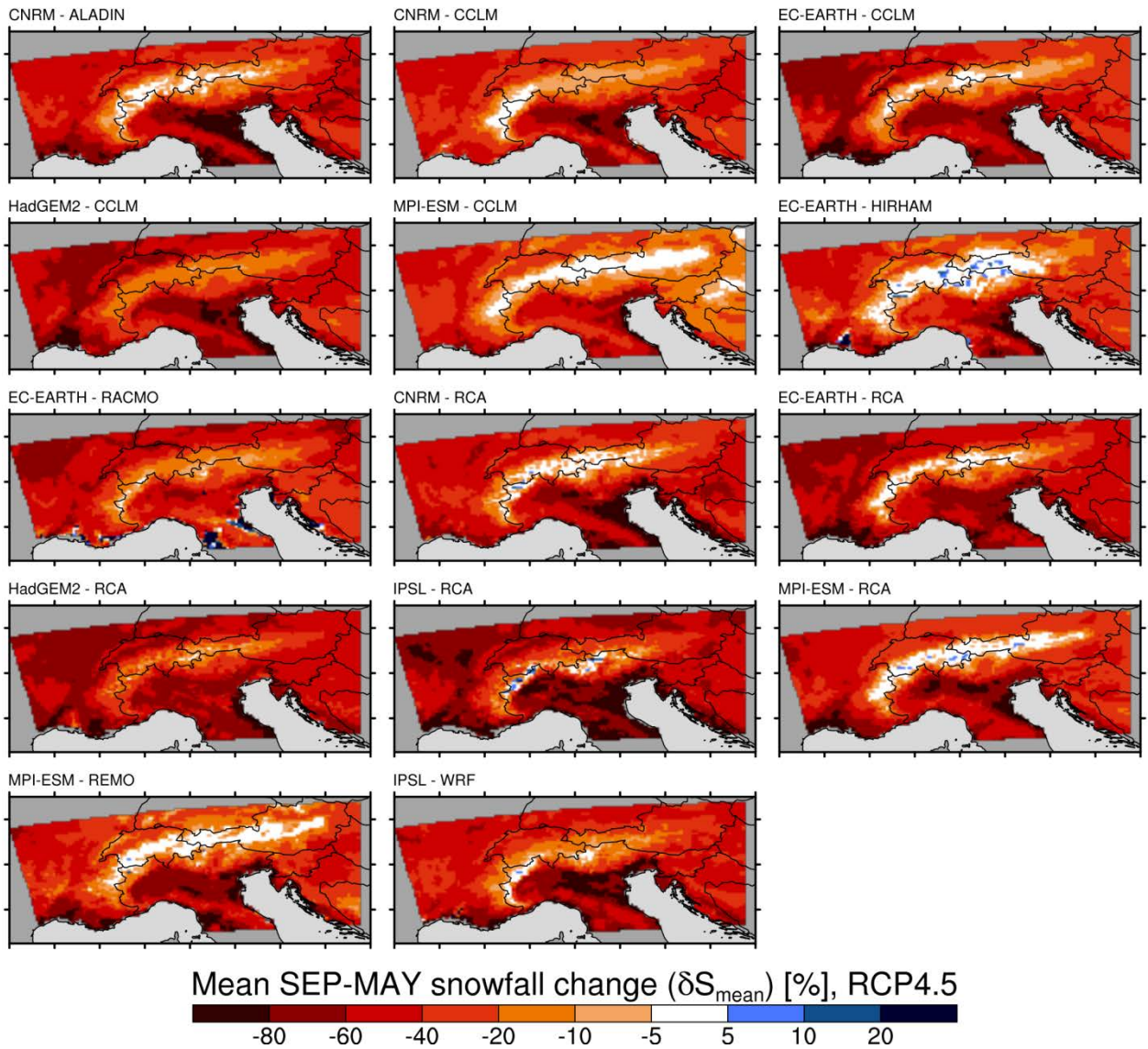


Figure S5 Spatial distribution of relative changes (SCEN period 2070-2099 with respect to CTRL period 1981-2010) in mean September-May snowfall, δS_{mean} , for RCP4.5 and for the 14 snowfall separated + bias corrected RCM simulations ($\text{RCM}_{\text{sep+bc}}$).

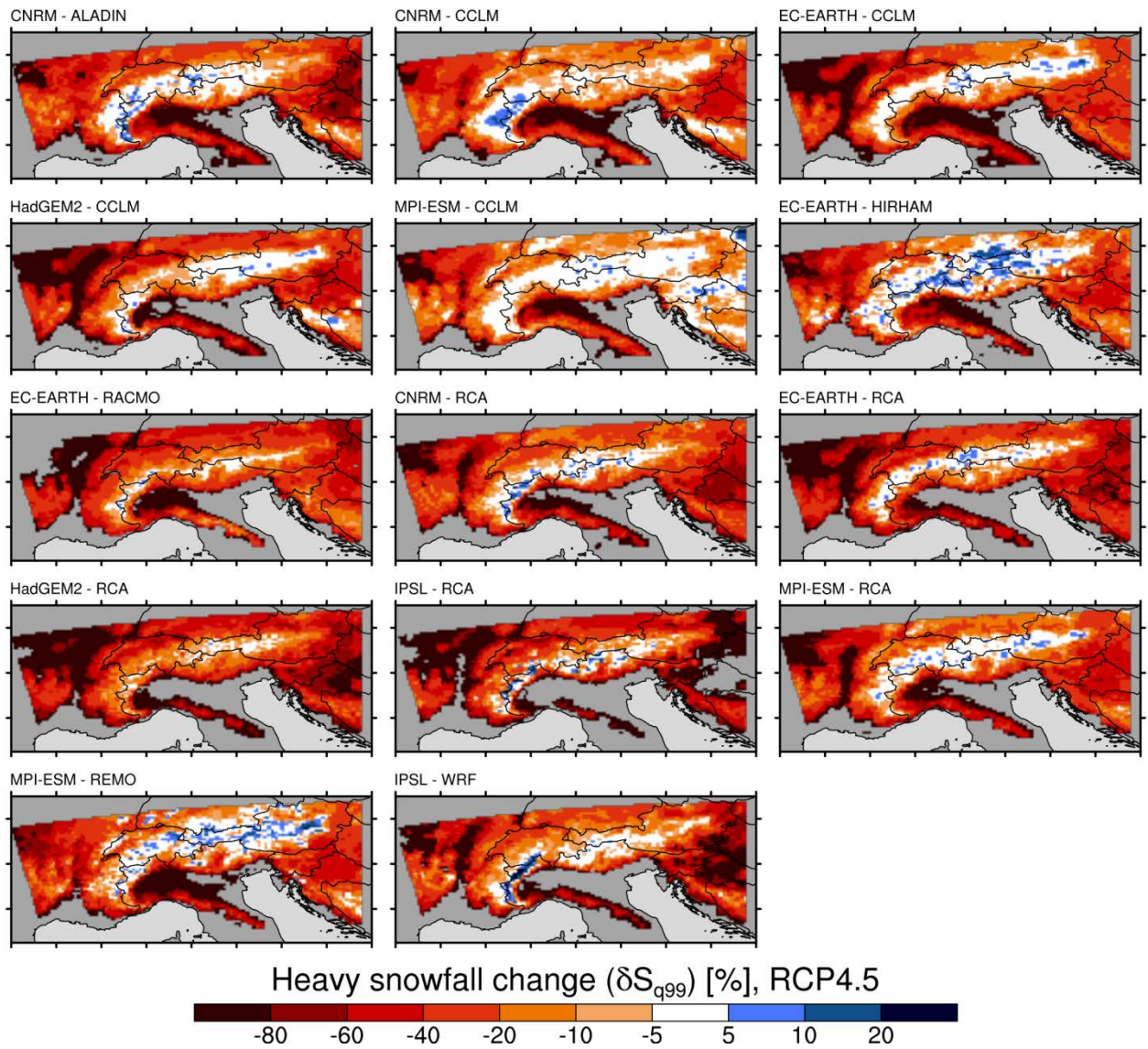


Figure S6 Spatial distribution of relative changes (SCEN period 2070-2099 with respect to CTRL period 1981-2010) in heavy snowfall, δS_{q99} , for RCP4.5 and for the 14 snowfall separated + bias corrected RCM simulations (RCM_{sep+bc}).

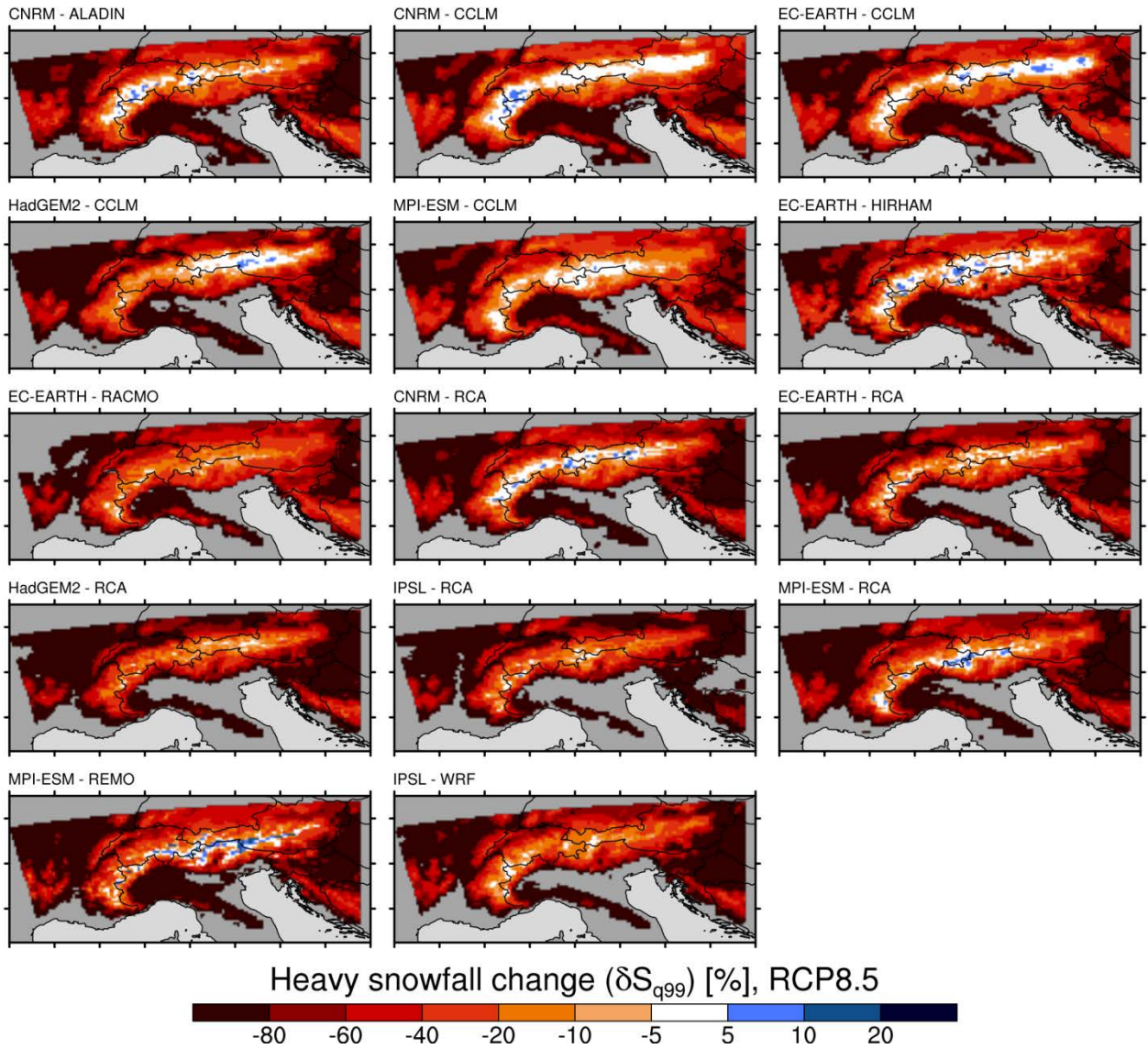


Figure S7 Spatial distribution of relative changes (SCEN period 2070-2099 with respect to CTRL period 1981-2010) in heavy snowfall, δS_{q99} , for RCP8.5 and for the 14 snowfall separated + bias corrected RCM simulations (RCM_{sep+bc}).

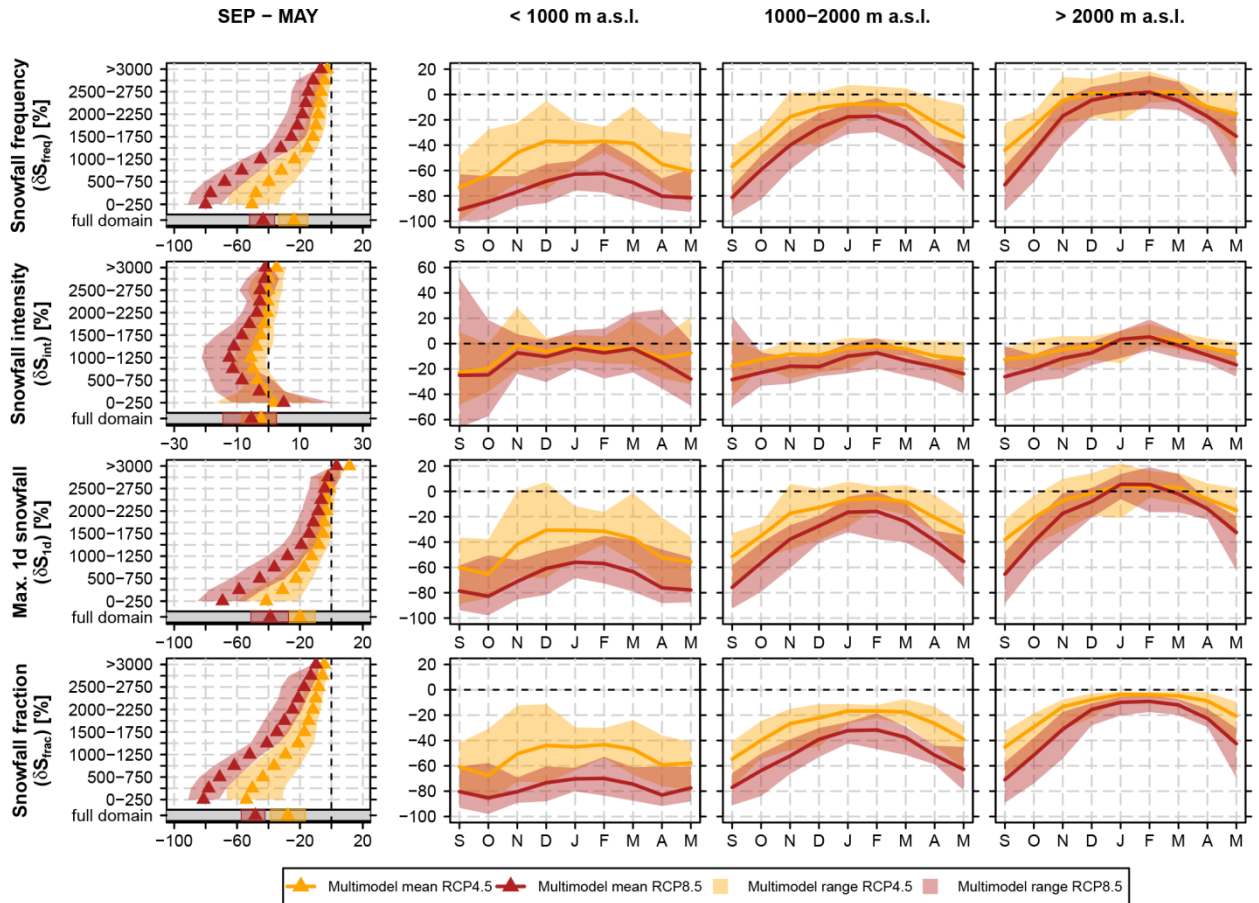


Figure S8 Relative changes (SCEN period 2070-2099 with respect to CTRL period 1981-2010) of max. 1 day snowfall, δS_{1d} , snowfall frequency, δS_{freq} , snowfall intensity, δS_{int} , and snowfall fraction, δS_{frac} , based on the 14 snowfall separated + bias corrected (RCM_{sep+bc}) RCM simulations for RCP4.5 and RCP8.5, each. The first column shows the mean September-May snowfall index statistics vs. elevation while monthly snowfall index changes (spatially averaged over the elevation intervals <1000 m.a.s.l., 1000 m a.s.l.-2000 m a.s.l. and >2000 m a.s.l.) are displayed in columns 2-4.